

Realtime Redundancy Allocation for Time-Varying Underwater Acoustic Channels

Beatrice Tomasi^{*}, Daniele Munaretto^{*} James C. Preisig[‡], Michele Zorzi^{*}

^{*}DEI, University of Padova — Via G. Gradenigo, 6/B, Padova, Italy

[‡]AOPE, Woods Hole Oceanographic Institution — 266 Woods Hole Rd., Woods Hole, MA, USA

{tomasibe,munaretto,zorzi}@dei.unipd.it jpreisig@whoi.edu

ABSTRACT

In this paper, we jointly address reliability and energy-efficiency in underwater acoustic (UWA) communications by proposing optimal redundancy allocation over time-varying conditions in a communication link. To do so, we use recent results on tight approximation of codeword error probability in the finite block-length regime. First, we propose and evaluate an optimization framework. Then, we design a realtime algorithm, able to allocate the redundancy in a point-to-point link, without adding control messages. We evaluate the performance of the proposed algorithm by considering both rapidly and slowly time-varying experimental channel conditions. Finally, we compare the performance of our algorithm with that obtained in a fixed rate coding scheme. Results show that the proposed redundancy allocation scheme is more efficient than constant allocation schemes under different channel conditions.

Keywords

Underwater acoustic communications, redundancy allocation, energy-efficiency, reliability.

1. INTRODUCTION

The recent development and employment of autonomous underwater vehicles, underwater sensors, and acoustic buoys motivate the interest in the design of reliable and energy-efficient underwater acoustic (UWA) communication strategies. On the one hand, reliable communications translate into an efficient utilization of the available bandwidth, which is a scarce resource in the UWA channel. On the other hand, energy-efficiency makes it possible to extend the lifetime of the aforementioned devices, which are usually battery-powered. Since transmission is the most energy consuming activity of an acoustic modem [1,2], energy can be saved by reducing as much as possible unsuccessful transmissions and the amount of unnecessary redundancy.

Following this reasoning, in this paper we propose an optimization framework and a realtime algorithm, able to jointly address reliability and energy-efficiency over time-varying conditions in a communication link. For the sake of simplicity, we model the UWA channel as a time-varying Binary Symmetric Channel (BSC)

and we support this assumption by showing experimental UWA channel conditions and the corresponding communications performance. Moreover, we compute the amount of redundancy which maximizes a metric, suitable for representing how efficiently the information is encoded in terms of both spectral efficiency and energy consumption. Furthermore, we design a realtime algorithm, able to allocate the precomputed optimal amount of redundancy. Finally, we evaluate its performance in both rapidly and slowly time-varying channel conditions, such as those measured during the KAM11 experiment [3].

As widely investigated in the past few years for terrestrial wireless communications, e.g., see [4–8], energy saving can be achieved by designing scheduling schemes characterized by low-power and long (low-rate) transmissions. However, these energy-efficient transmission schemes assume block-fading or additive white Gaussian noise channel models, which may not be suitable for representing the doubly selective UWA channel over intervals of time covered by long packets. Therefore, further analysis and validation is needed to tailor these energy-efficient schemes to UWA communications.

In the literature, the problem of reliable UWA communications has been studied, e.g., in [9–14]. In particular, the authors of [9,10] investigate the performance of rateless coding schemes used for broadcast communications. In [11], the authors study the trade-off between delay and reliability in a multi-hop sensor network. The authors of [12] perform a simulation study on the reliability achieved by the proposed Automatic Repeat reQuest (ARQ) technique, tailored to UWA communications. Even though these studies provide insight on the reliability associated to a multi-user channel in different networking scenarios, the presented results are limited to the case of time-invariant channel fading, since only the dependence on distance is considered.

In contrast to this previous work, we focus on the unreliability due to time-variability in an acoustic link. In particular, we design and evaluate a framework which allocates in realtime the redundancy required to protect UWA transmissions, based on limited channel side information (CSI). This CSI is provided by either an acknowledgement (ACK) or not-acknowledgement (NACK) sent by the receiver to the transmitter, upon the receipt of a packet.

In [14], the authors design a super-Nyquist modulation and rateless coding scheme suitable for doubly-selective underwater acoustic channels. However, they do not explicitly consider optimality allocating the redundancy to decrease the number of retransmissions. The authors of [17] propose a rateless coding scheme, whose soliton distribution adapts to the fading conditions and which runs based on limited CSI (ACK/NACK) available at the transmitter. They show that this adaptive rateless code outperforms the standard rateless codes in terms of throughput. In this work a similar adaptive coding scheme is considered. However, here we calcu-

Permission to make digital or hard copies of all or part of this work for personal or classroom use is granted without fee provided that copies are not made or distributed for profit or commercial advantage and that copies bear this notice and the full citation on the first page. To copy otherwise, to post on servers or to redistribute to lists, requires prior specific permission and/or a fee.

Copyright 20XX ACM X-XXXXX-XX-X/XX/XX ...\$10.00.

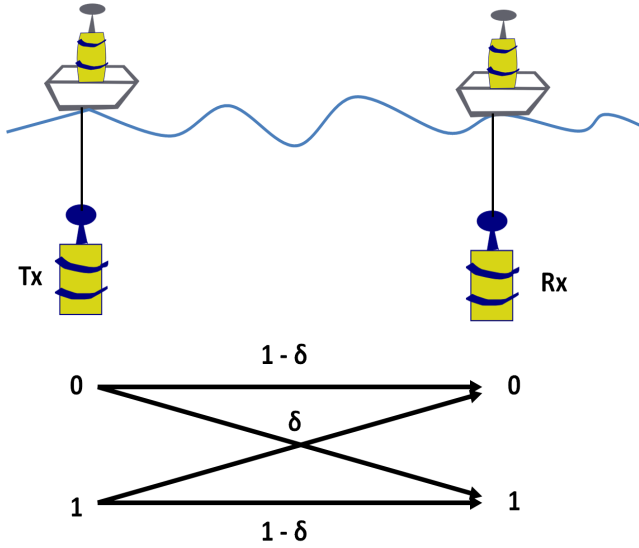


Figure 1: Typical UWA scenario, single-user communication channel. Below, the corresponding binary symmetric channel, with crossover probability δ .

late in real time the precomputed optimal amount of redundancy without introducing extra control messages.

The structure of the paper is summarized as follows. In Sec. 2, we present the considered scenario and channel model. In the same section, we define a metric representing the encoding efficiency. In Sec. 3, we formulate the optimization problem, from which we compute the amount of redundancy that maximizes the aforementioned metric. In Sec. 4, by leveraging on these results, we design a realtime algorithm, able to allocate the redundancy in an actual UWA scenario and we evaluate its performance by considering both rapidly and slowly time-varying channel conditions. Sec. 5 concludes the paper.

2. SYSTEM MODEL

The scenario consists of an acoustic communication system as represented in Fig. 1, where a single transmitter-receiver pair is considered and no multi-user interference occurs. This is an appropriate model for a deterministic medium access control scheme, such as Time Division Multiple Access (TDMA), which has been proposed and studied for UWA networking scenarios [15,16]. Moreover, we assume a fixed traffic generation rate. In fact, differently from the power control schemes that aim at maximizing the amount of information for a given average power constraint, here we aim at maximizing the spectral efficiency per transmission, subject to a fixed amount of information to be successfully transmitted, which is a practical scenario for UWA communications.

More specifically, we consider the scenario of an adaptive coding scheme, which can adjust the amount of redundancy per transmission. At each transmission, the amount of redundancy is chosen according to the channel conditions, by solving the optimization problem presented in Sec. 3 with the algorithms proposed in Sec. 4.

2.1 Metric and channel model

In the following, we indicate the amount of information to be transmitted and the corresponding redundancy as x and y , respectively. The overall codeword length, n , is given by $n = x + y$. The

efficiency metric to be maximized is defined as:

$$\eta(x, y, \epsilon) = \frac{x(1 - \epsilon)}{x + y}, \quad (1)$$

where ϵ is the codeword error probability. This error probability (and its approximation) was derived in [18] for several channel models in the finite block-length regime. In particular, in this paper, we consider the BSC model, represented in Fig. 1. The choice of this model is mainly due to the fact that it makes it possible to obtain close-form results, and therefore simplifies the analysis of the system, while also matching the collected experimental data for a point-to-point UWA channel sufficiently well.

The efficiency metric, η , represents the trade-off between reliability, indicated by the factor $1 - \epsilon$, and spectral efficiency, expressed by the ratio $x/(x + y)$. In fact, η is a decreasing function of y , and an increasing function of $1 - \epsilon$. However, $1 - \epsilon$ itself is an increasing function of y , thus revealing a trade-off, which depends on how rapidly ϵ decreases as redundancy increases. This trade-off gives rise to an optimum value y_{opt} that maximizes η , and should be used to optimally allocate redundancy. In fact, transmitting more redundancy would only increase the energy consumption at the transmitter, since unnecessary bits would be sent. On the other hand, if insufficient redundancy is transmitted, the receiver will request a retransmission by sending a NACK, thus increasing both energy consumption and delay.

The codeword error probability, ϵ , depends on x , y , and the channel conditions. In case of a BSC model, fully described by the crossover probability δ , ϵ depends on x , y , and δ . In particular, in [19] and in [18, pag. 51-54] the author derives an upper bound for the achievable rate, $\log M(\epsilon, n)$, from which we derive the expression for ϵ as a function of x , y , and $\delta \notin \{0, \frac{1}{2}, 1\}$, which can be written as:

$$\epsilon(x, y, \delta) = Q\left(\frac{nC(\delta) - x + \frac{1}{2} \log n}{\sqrt{nV(\delta)}}\right), \quad (2)$$

where

$$Q(z) = \frac{1}{\sqrt{2\pi}} \int_z^\infty e^{-\frac{w^2}{2}} dw. \quad (3)$$

The capacity, $C(\delta)$, of a BSC with crossover probability δ is:

$$C(\delta) = 1 - h(\delta) \quad (4)$$

where $h(\delta)$ is the entropy equal to:

$$h(\delta) = -\delta \log(\delta) - (1 - \delta) \log(1 - \delta) \quad (5)$$

whereas $V(\delta)$ is called channel dispersion, defined in [18, pag. 12], and in case of a BSC becomes:

$$V(\delta) = \delta(1 - \delta) \log^2 \frac{1 - \delta}{\delta}. \quad (6)$$

This quantity indicates the coefficient, V in the approximation valid for different channel models:

$$\log M(n, \epsilon) = nC - \sqrt{nV}Q^{-1}(\epsilon) + O(\log n). \quad (7)$$

The rationale behind the choice of the BSC model lies in its simplicity as well as in its suitability to provide insights on how to optimally allocate the redundancy over subsequent packets affected by time-varying channel conditions. Such approximation is verified using experimental data. However, it is also worth noticing that our framework is independent of the channel model, as soon as the codeword error probability can be expressed as a function

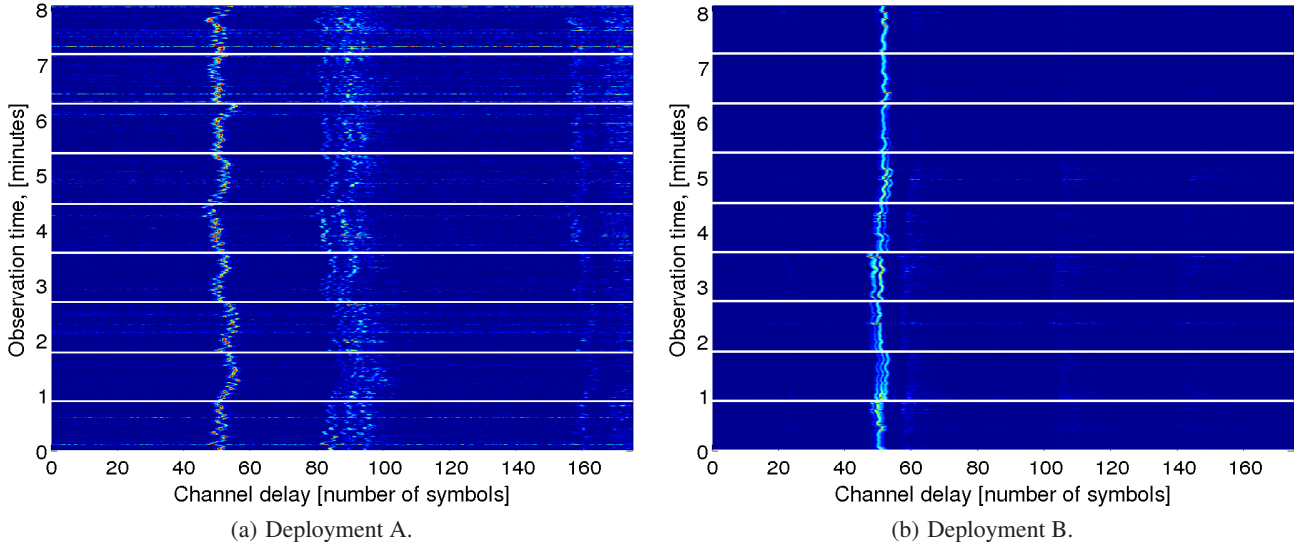


Figure 2: Time series of the amplitude estimates of the channel impulse response, during Julian dates 181 at 4 p.m. (UTC) (deployment A) and 187 at 4 a.m. (UTC) (deployment B). The x -axis corresponds to the channel delay, whereas the y -axis represents the recording time, which spans 9 minutes.

of the channel conditions, x and y . Understanding which model would be more accurate for real underwater acoustic communications is under study. In order to qualitatively support this model, we present some experimental results in terms of Signal to Interference plus Noise Ratio (SINR)¹ and Bit Error Rate (BER) during two different deployments, subject to different time-varying channel conditions.

2.2 Experimental channel evaluation

In order to support the suitability of the BSC model, we analyze a set of acoustic signals transmitted under water and collected during the KAM11 experimental trial [3]. In particular, we focus on a train of nine almost one-minute long acoustic signals, BPSK modulated at center frequency 13 kHz and rate 6250 bps. We consider the signals recorded at 3 km from the transmitter. Furthermore, in order to show different time-varying conditions, we present the results for two deployments, where the shallowest transducer was deployed at A) 15 m and B) 45 m below the surface. The transmitter was 45 m below the surface for both deployments. We remark that these two deployments also refer to different time intervals of the experimental campaign.

However, since consistent channel behaviors were observed in each deployment for several consecutive days, and the two deployments were tested in adjacent time periods, we may conclude that the critical factor affecting the observed behavior is the different position of the receiver, rather than the time at which the measurements were taken. As an example, we represent in Figs. 2(a) and 2(b) the time series of the amplitude of the channel impulse responses for A and B, respectively.

When the receiver moves due to surface fluctuations, this produces impulse noise represented by tiny horizontal lines in the channel impulse response estimates in Fig. 2. In deployment A, since the receiver is closer to the surface, this effect is more visible (see

¹Note that interference here means Inter-Symbol Interference (ISI), since the considered communication system is ultra-wide band in a communication link.

Fig. 2(a)), whereas in deployment B, as shown in Fig. 2(b), the channel exhibits a more stable structure of arrivals and the impulse noise is negligible. We remark that the horizontal thick white lines in Figs. 2(a) and 2(b), separating each minute of observation, represent the silent time interval between subsequent transmissions of the acoustic signals.

Similar observations hold for Figs. 3(a) and 3(b), representing the time series of the BER, δ , and of the SINR, estimated over subsequent chunks of the transmitted signal, 5190 symbols long, of which 1100 are used for synchronization and initialization of the Decision Feedback Equalizer (DFE)². We remark that the quantization effect in the low BER regime (below 10^{-3}) is due to the fact that we estimate BER over limited sized packets. Whenever the receiving system is unable to correctly synchronize and to estimate the channel, the chunks are dropped from the analysis.

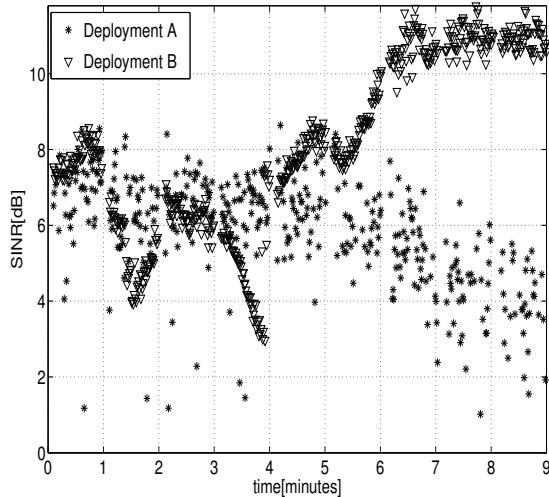
As a final note, we want to stress that the BSC model could be more accurate for deployment B, for which slower time-varying channel conditions were measured. In fact, if a packet lies within a channel coherence time, the error statistics are time-invariant, and thus can be represented by a single crossover probability δ . On the other hand, if we consider longer packets, e.g., 10 s, which possibly span multiple channel coherence times, sometimes of the order of a few seconds, a more complex model, such as a Markov model with memory, should be taken into account. This extension is left for future work.

3. OPTIMIZATION PROBLEM

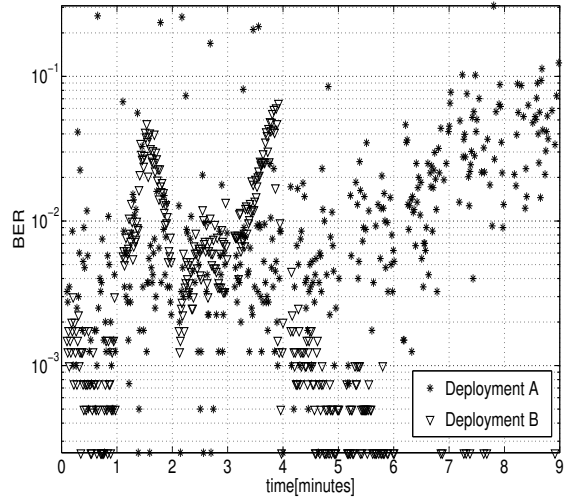
In this section, we develop the optimization framework that, based on a given number of information bits x and on the bit error rate δ , infers the optimal amount of required redundancy as follows:

$$y_{opt} = \underset{y}{\operatorname{argmax}} \eta(x, \epsilon, y), \quad (8)$$

²The equalizer is used in training mode. It combines the signals measured at four channels spanning half a meter of the column water. Moreover, in order to compensate for time-varying channel durations, we adapt accordingly the length of the feedback filter.



(a) SINR time series



(b) BER time series (y -axis is in logarithmic scale)

Figure 3: SINR and BER time series, from the KAM11 experimental campaign during Julian dates 181 (4 p.m.) and 187 (4 a.m.), indicated with stars and triangles, respectively.

where x is constant and application-dependent and y is chosen so as to maximize $\eta(x, \epsilon, y)$, under given channel conditions. In order to find a maximizer, we study the sign of the first derivative of $\eta(x, \epsilon, y)$ with respect to y . Such derivative can be expressed as:

$$\frac{\partial \eta}{\partial y} = \partial_y \left(\frac{x(1 - \epsilon(x, y, \delta))}{x + y} \right) \quad (9)$$

$$= \frac{-(x + y)x\partial_y \epsilon(x, y, \delta) - x(1 - \epsilon(x, y, \delta))}{(x + y)^2}. \quad (10)$$

In the numerator, the first term has only positive factors, with the exception of $\partial_y \epsilon(x, y, \delta)$, which is negative, since ϵ is a strictly decreasing function of y . This makes the first term positive. Conversely, $x(1 - \epsilon(x, y, \delta))$ is non-negative, since $x > 0$ and $\epsilon(x, y, \delta) \in [0, 1]$, thus making the second term non-positive. These considerations highlight that there exists a trade-off between the two terms, which determine the sign of $\partial_y \eta(x, y, \delta)$ as a function of y .

3.1 Numerical results

We numerically evaluate the solutions provided by the optimization framework. In particular, we consider x varying in the interval $[200, 1000]$, with an increment of 50 bits, and δ spanning the interval $[10^{-3}, 0.1]$, with increments of 0.005. In the considered range for δ , there exists a y_{opt} maximizing η (an example of this behavior is shown in Fig. 4). For very small values of δ , $\eta(x, y, \delta)$ turns out to be a monotonically decreasing function of y , so that the optimal value is $y_{opt} = 0$ and no redundancy should be used (i.e., it is better to take a chance and then retransmit whenever needed instead of investing resources to provide a priori error protection). On the other hand, for values of δ close to 0.5 the maximum efficiency would occur for very large values of y , which would lead to impractical values of the packet size. In this case one may either limit y to the maximum value allowed, or refrain from transmission altogether.

As an example of the obtained results, in Fig. 4, we show $\eta(x, y, \delta)$ and its first derivative with respect to y , when x is 200 and δ is 0.046. It can be noticed that η slowly increases for small y ($\partial_y \eta \sim 0$), whereas as y increases, it also steeply increases since the successful decoding probability tends to 1 ($\partial_y \eta > 0$). After-

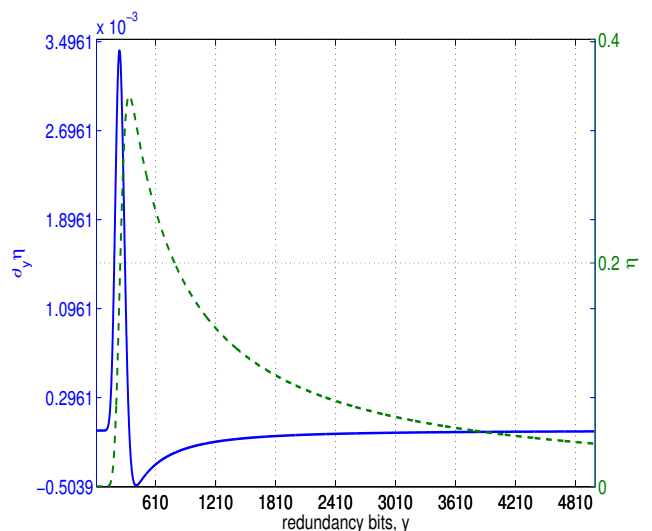


Figure 4: η and its first derivative are represented in green (dashed) and blue curves, respectively. In this case, $x = 200$ bits and $\delta = 0.046$.

wards, η decreases for larger values of y ($\partial_y \eta < 0$).

In Figs. 5 and 6, we show the computed y_{opt} for the considered intervals of x and δ . In particular, each curve in Fig. 5 is obtained by cutting the 3D plot in Fig. 6 with a vertical plane for a constant value of x . We make use of these results in the realtime algorithm for redundancy allocation as they become precomputed values of y_{opt} in a look-up table, as explained in Sec. 4.

4. ALGORITHMS AND EVALUATION

In this section, we design an allocation algorithm, starting from the transmitter side, which is in charge of allocating the redundancy

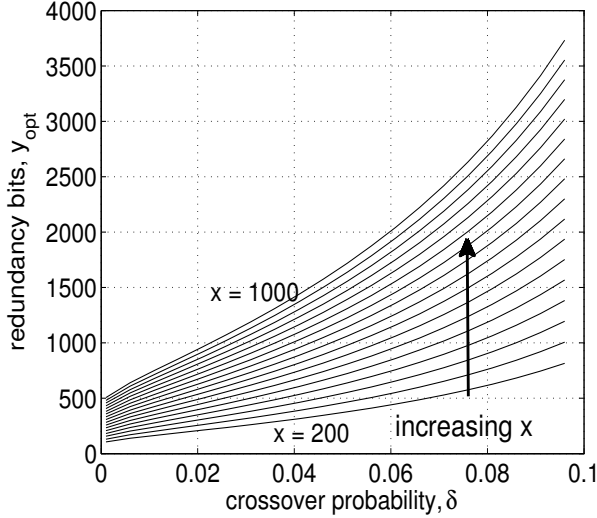


Figure 5: The y -axis represents the optimal number of redundancy bits, obtained from the optimization framework, for varying x (represented by the different curves) and δ (in the x -axis).

Algorithm 1 Algorithm to compute the optimal FEC, as for Sec. 3.

Input: δ bit error rate, and x information bits;

Computation optimal FEC, y_{opt} :

- $V(\delta) = \delta(1 - \delta)\log^2\left(\frac{1-\delta}{\delta}\right)$;
- $C(\delta) = \log 2 - \delta\log\frac{1}{\delta} - (1 - \delta)\log\frac{1}{1-\delta}$;
- Compute $y_{opt} = \underset{y}{\operatorname{argmax}} \eta(y)$;

Output: y_{opt} .

based on the ACK/NACK fed back by the receiver.

Algorithm 1 is responsible for computing the optimal redundancy needed for the next transmission based on δ , the measured bit error rate, and x , the number of information bits to be transmitted (see the optimization problem in Sec. 3). Beforehand, in an offline fashion, the operator should build a look-up table, containing couples of BER, δ , and the corresponding optimal amount of Forward Error Correction (FEC), y_{opt} . The number of entries is fixed based on the granularity and range of the levels of quality of service required by the application. The more the couples, the finer the tuning of the redundancy to be allocated in the packets to be transmitted. As an extreme case, one entry in the table corresponds to fixing a constant packet length for any value of δ .

In detail, in order to pre-build the look-up table at the transmitter side, algorithm 1 runs over a set of pre-computed δ s (offline computation). For each δ , it calculates the dispersion $V(\delta)$ and the capacity $C(\delta)$, and thus the corresponding optimal number of redundant bits y_{opt} . This procedure is repeated for each entry of the look-up table.

At this point, it is worth noticing that, since δ cannot be easily made available to the transmitter, during the realtime redundancy allocation phase, we need to map somehow a metric, e.g., the SINR, that the transmitter can estimate to the corresponding value of δ . In order to do so, we preset a mapping function between the values of SINR and BER, estimated during an initial channel probing session. As an example, in Fig. 7 we show the estimates of the couples (SINR, BER) for deployment A, KAM11. This plot is representa-

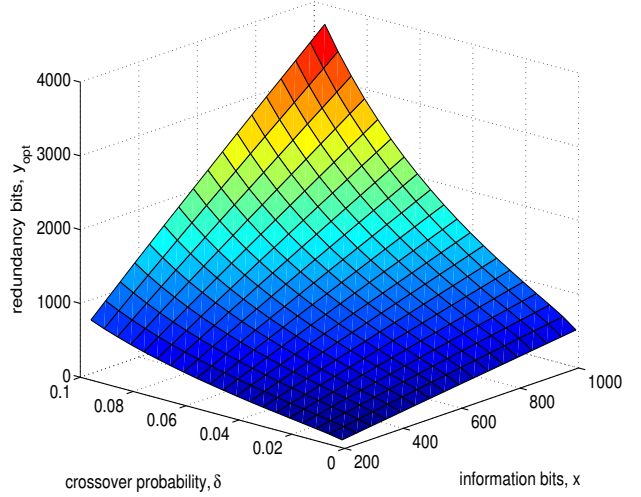


Figure 6: Surface plot of the numerical results obtained for $x \in [200, 1000]$, and $\delta \in [10^{-3}, 0.1]$.

Algorithm 2 Algorithm at the transmitter side.

Input: R channel realizations, BPSK modulation, L_{packet} maximum packet length, x information bits and look-up table (BER_i, FEC_i);

Procedure:

- Estimation of SINR upon chirp receipt;
- Mapping of SINR to BER, getting δ ;
- Selection of the i -th level from the look-up table (BER_i, FEC_i), for which BER_i is the closest value to the measured δ :
- $i = \underset{j}{\operatorname{argmin}} |\delta - BER_j|$;
- Selection of FEC_i ;

if $L_{packet} \geq (x + FEC_i)$ **then**

Output: send a packet of length $x + FEC_i$.

else

Output: send probe packet.

end if

tive of a general behavior observed over most of the experimental data. Thanks to this behavior, the mapping function is inferred by associating to each SINR the corresponding average BER value.

Algorithm 2, implemented at the transmitter side, is responsible for allocating the redundancy during subsequent transmissions. In particular, the transmitter is aware of the SINR seen at the receiver, $\hat{\gamma}$. This measure of the channel quality can be collected through a chirp sent by the receiver. We propose to use, e.g., an ascending chirp as ACK and a descending chirp as NACK. This solution is more efficient than sending a feedback message, containing only one bit of ACK/NACK and including large overhead in order to cope with the harsh UWA channel conditions. Once the SINR is measured, it can be mapped to an average BER, δ , as aforementioned. Finally, the transmitter selects the corresponding value of FEC, thus resulting into a new packet. If the total length exceeds the maximum allowed packet length, denoted as L_{packet} , no transmission is performed, otherwise the packet is sent out.

At the transmitter side, we can also distinguish two cases, according to whether the look-up table is computed i) online, and ii) offline. In case i), every T_{clock} ticks, the receiver sends a train of

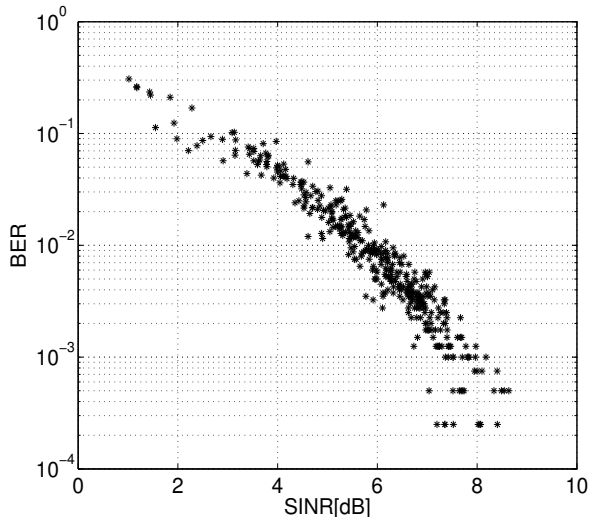


Figure 7: BER vs. SINR for the collected data during Julian date 181 (4 p.m.), deployment A.

probing signals, known at the transmitter side, in order to be able to estimate the corresponding δ . In case ii), before deployment each link is characterized through a look-up table, in the same way but for longer periods of time.

During the communication session, the receiver’s tasks are to decode the packet and send an ACK if the decoding is successful, or a NACK otherwise. It can be noticed that the proposed communication system leaves the burden of selecting the suitable amount of redundancy as well as the channel probing responsibility to the transmitter side. This is justified by the fact that a more complex feedback procedure (other than ACK/NACK, e.g., SINR estimation at the receiver fed back to the transmitter) may not pay off in terms of performance in the presence of long propagation delays that would make the feedback too outdated to be useful.

4.1 Results

In this section, we evaluate the proposed redundancy allocation algorithm by means of simulation. In particular, we consider the experimental data shown in Figs. 2(a) and 2(b), which are representative of the different deployment depths.

First, we compute a finer SINR time series over the 9 minutes. Each SINR is estimated by processing packets consisting of 1300 symbols (208 ms), so as to make such time series suitable for the simulation of multiple packet transmissions. At every simulation run, we read the estimated SINR, based on which we compute the proper amount of redundancy y_{opt} . Then, we run the receiving decoding processing over the chunk of data immediately subsequent to the time of the SINR estimate. If the currently measured bit error rate, $\delta(i)^3$, is greater than the BER assumed in the computation of y_{opt} , the packet is considered unsuccessfully decoded. At the next iteration, the subsequent considered SINR is separated in time by the last packet duration plus the round trip time (which here is 4

³We remark that we focus on a general result, independent of the type of implemented encoder/decoder, therefore here we do not implement a specific coding scheme.

	$\eta_{0.001}$	η	$\eta_{0.1}$	average SINR dB
Dep. A	0.028	0.318	0.201	5.8459
Dep. B	0.371	0.465	0.207	8.1168

Table 1: Results in terms of η , $\eta_{0.001}$, and $\eta_{0.1}$ evaluated over deployments A and B.

seconds). In this way, we could estimate the metric η , as:

$$\hat{\eta} = \frac{1}{N} \sum_{i=1}^N \mathbf{1}\{\delta(i) \leq BER(i)\} \frac{x}{x + y(i)} \quad (11)$$

where N is the number of iterations and $\mathbf{1}\{\delta(i) \leq BER(i)\}$ is the indicator function. Similarly, we compute η in two cases of constant packet lengths obtained for i) $BER = 10^{-3}$, and ii) $BER = 0.1$. We denote the obtained evaluation of η as i) $\eta_{0.001}$ and ii) $\eta_{0.1}$.

The results are shown in Table 1. It can be noticed that the proposed optimal allocation provides the highest encoding efficiency for both deployments, which have different communication channel qualities, as highlighted in the last column. The constant allocation assuming the smallest BER provides higher efficiency than the other constant allocation for deployment B, in which the channel conditions were favorable. Vice-versa, for deployment A, the more robust constant allocation outperforms the other. In both cases, an adaptive redundancy allocation, based on the proposed BSC model, would gain around 58% and 25%, with respect to the corresponding suboptimal constant allocation in deployment A and B, respectively.

These results motivate further analysis on how to encode larger packets, which are more sensitive to the time-varying conditions of the arrival structure of the channel.

5. CONCLUSIONS AND FUTURE WORK

In this paper, we built an optimization framework, well supported by experimental evidence. We used a BSC channel model to reflect in a simple way but without loss of generality the channel conditions measured in the collected data. We defined a metric representing how efficiently the information is encoded in terms of both spectral efficiency and energy consumption and we formulated the optimization problem to maximize such metric. Finally, we designed a realtime algorithm to compute the redundancy required in a UWA communication link.

The presented study and results pave the way for future work. In particular, we plan to evaluate the efficiency of the proposed algorithm as a function of average SINR and channel coherence times, estimated in a more extensive data set. Moreover, we want to investigate how to allocate in realtime the redundancy over longer packets, for which Markov channel models should be validated. As a final goal, we want to understand whether short or long packets are more efficient (in terms of both bandwidth and energy) in UWA communication systems.

Acknowledgment

This work was supported by ONR under Grants no. N00014-10-10422, N00014-07-10738 and N00014-11-10426, and by the European Commission under the Seventh Framework Programme

(Grant Agreement 258359 - CLAM).

6. REFERENCES

- [1] WHOI umodem, "<http://acomms.who.edu/umodem/>".
- [2] Evologics acoustic modems, "<http://www.evologics.de/en/products/acoustics/index.html>".
- [3] W.S. Hodgkiss and J.C. Preisig, "Kauai Acomms MURI 2011 (KAM11) Experiment," in *Proc. 11th European Conference on Underwater Acoustics (ECUA 2012)*, pp. 993-1000, 2012.
- [4] E. Uysal-Biyikoglu and B. Prabhakar and A. El Gamal, "Energy-efficient packet transmission over a wireless link," in *IEEE/ACM Transactions on Networking*, vol. 10, no. 4, pp. 487-499, 2002.
- [5] E. Uysal-Biyikoglu and A. El Gamal, "On adaptive transmission for energy efficiency in wireless data networks," in *IEEE Transactions on Information Theory*, vol. 50, no. 12, pp. 3081-3094, 2004.
- [6] M. Zafer and E. Modiano, "Optimal rate control for delay-constrained data transmission over a wireless channel," in *IEEE Transactions on Information Theory*, vol. 54, no. 9, pp. 4020-4039, 2008.
- [7] J. Lee and N. Jindal, "Energy-efficient scheduling of delay constrained traffic over fading channels," in *IEEE Transactions on Wireless Communications*, vol. 8, no. 4, pp. 1866-1875, 2009.
- [8] R. Srivastava and C.E. Koksal, "Energy optimal transmission scheduling in wireless sensor networks," in *IEEE Transactions on Wireless Communications*, vol. 9, no. 5, pp. 1550-1560, 2010.
- [9] P. Casari and M. Rossi and M. Zorzi, "Towards optimal broadcasting policies for HARQ based on Fountain codes in underwater networks," in *Proceedings of IEEE/IFIP WONS*, 2008.
- [10] P. Casari and A. F. Harris III, "Energy-efficient reliable broadcast in underwater acoustic networks," in *Proceedings of ACM WUWNet*, 2007.
- [11] W. Zhang and U. Mitra, "A delay-reliability analysis for multihop underwater acoustic communication in *Proceedings of ACM WUWNet*, 2007.
- [12] Z. Haojie and T. Hwee-Pink and A. Valera and B. Zijian, "Opportunistic ARQ with bidirectional overhearing for reliable multihop underwater networking," in *Proceedings of IEEE OCEANS*, Sydney, May, 2010.
- [13] Q. Fengzhong and L. Yang, "Rate and reliability oriented underwater acoustic communication schemes," in *Proceedings of IEEE DSP/SPE*, 2009.
- [14] U. Erez and G. Wornell, "A super-Nyquist architecture for reliable underwater acoustic communication," in *Proceedings of Conference on Communication, Control, and Computing (Allerton)*, pp. 469-476, 2011.
- [15] L. Badia and M. Mastrogiovanni and C. Petrioli and S. Stefanakos and M. Zorzi, "An optimization framework for joint sensor deployment, link scheduling and routing in underwater sensor networks" in *Proceedings of ACM WUWNet*, 2006.
- [16] K. Kredo and P. Djukic and P. Mohapatra, "STUMP: Exploiting Position Diversity in the Staggered TDMA Underwater MAC Protocol", in *Proceedings of IEEE INFOCOM*, 2009.
- [17] N. Bonello and Z. Rong and C. Sheng and L. Hanzo, "Reconfigurable rateless codes," in *IEEE Transactions on Wireless Communications*, vol. 8, no. 11, pp. 5592-5600, 2009.
- [18] Y. Polyanskiy, "Channel coding: non-asymptotic fundamental limits," *Ph.D. dissertation*, Princeton Univ., Princeton, NJ, USA, 2010.
- [19] Y. Polyanskiy and H. V. Poor and S. Verdú, "Channel coding rate in the finite blocklength regime," in *IEEE Transactions on Information Theory*, vol. 56, no. 5, pp. 2307-2359, 2010.
- [20] Y. Polyanskiy and H. V. Poor and S. Verdú, "Dispersion of the Gilbert-Elliott channel," in *IEEE Transactions on Information Theory*, vol. 57, no. 4, pp. 1829-1848, 2011.